water

MDPI

Article

Oxidation of an Azo-Dye via the Photo-Fenton Process under Heterogeneous and Homogeneous Conditions

Abel Riaza-Frutos [1], Agata Egea-Corbacho [1,2,*], Manuel A. Manzano [1] and José María Quiroga [1]

[1] Department of Environmental Technologies, Faculty of Marine and Environmental Sciences, University of Cadiz, 11510 Puerto Real, Spain
[2] Materials and Sustainability Group, Department of Engineering, Universidad Loyola Andalucía, 41704 Dos Hermanas, Spain
* Correspondence: agata.egea@uca.es

Abstract: In today's industries, a diversity of processes give rise to increasing numbers of non-biodegradable compounds that need to be degraded totally or transformed to other less toxic and/or more biodegradable compounds, before their discharge into the environment. One such compound chosen for this study is Orange II, a representative azo-dye that is widely used and easy to monitor in its degradation. The photo-Fenton process was used under heterogeneous and homogeneous conditions to study several different variables. At the end of this research, a comparative study was carried out between the two types of catalysis. It was observed that better results in primary degradation and mineralization were provided by homogeneous catalysis. The photo-Fenton process takes place effectively under heterogeneous and homogeneous catalysis conditions. The process is much faster under homogeneous conditions than under heterogeneous conditions (99.9 and 24% after 90 min, respectively, especially when only 2 ppm of iron in solution is required). Mineralization was observed through total organic carbon, through the variable C/Co as a function of time during photo-Fenton and Orange II degradation, and the data obtained for the final oxidation capacity are in agreement with the experimental percentages of mineralization. A linear fit was observed using the Chan–Chu kinetic model for heterogeneous and homogeneous catalysis. For heterogeneous catalysis, 56% mineralization was reached whereas the model predicts 63%. Regarding homogeneous catalysis, according to the model, 100% mineralization is reached because (1/σ) takes a value greater than 1 since the model calculates it on infinite time.

Keywords: oxidation; photo-Fenton; wastewater; azo-dye

check for updates

Citation: Riaza-Frutos, A.; Egea-Corbacho, A.; Manzano, M.A.; Quiroga, J.M. Oxidation of an Azo-Dye via the Photo-Fenton Process under Heterogeneous and Homogeneous Conditions. *Water* **2023**, *15*, 1787. https://doi.org/10.3390/w15091787

Academic Editors: Md. Nahid Pervez and Yingjie Cai

Received: 12 April 2023
Revised: 2 May 2023
Accepted: 5 May 2023
Published: 6 May 2023

Copyright: © 2023 by the authors. Licensee MDPI, Basel, Switzerland. This article is an open access article distributed under the terms and conditions of the Creative Commons Attribution (CC BY) license (https://creativecommons.org/licenses/by/4.0/).

1. Introduction

In the textile industry, the main pollutants are the dyes, which consist of one or more chromophore groups (groups of atoms with unsaturated connections that give color). There are approximately 12 chromophore groups, the most important being the azo-compounds (-N=N-) that include 60–70% of the textile dyes, followed by the quinones [1,2].

All the pollutants except the color can be reduced by conventional chemical and physical treatment methods. Consequently, the biggest problem with textile wastewaters is the color, produced by the residuals of dyes in the dyeing processes [3–5]. It has been found that some methods are either not viable or not completely effective in degrading water-soluble azo-dye; direct photolysis [6,7], coagulation–flocculation processes [4], and biological processes [8,9] are among these methods [10].

For this research, it was therefore decided to apply a variant of the Fenton process (Fenton, 1894) called photo-Fenton, which is included among the advanced oxidation processes (AOPs) [11,12]). Other authors have used Fe-doped zinc oxide (Fe-ZnO) and UV-A irradiation for the removal of two widely used antibiotics found in hospital wastewater with positive results [13]. Other authors have studied the synthesis of a β-FeOOH/polyaniline

heterogeneous catalyst for efficient photo-Fenton degradation of AOII dye [14]. Heterogeneous (iron fixed in perfluorinated membranes of Nafion®117) and homogeneous (dissolved iron ions) catalysis methods were used [15,16]. These membranes resist the attack of the hydroxyl radical and can thus be reused for further treatment.

The Fenton process [17] consists of the generation of the hydroxyl radical (HO•) by means of the reaction between ferrous ion and hydrogen peroxide (chemical reaction (1)). This radical is highly oxidizing and can react in an indiscriminate way with different organic compounds. The process does not need to be irradiated since it takes place rapidly due to the ferrous ion being recycled, as chemical reaction (2) indicates. However, if an illumination source is used (as in the photo-Fenton process), this increases the yield and rate of the reaction due to the increased effectiveness produced by the photo-reduction of the ferric to ferrous ion (chemical reaction (3)), where an extra hydroxyl radical is generated if the ferric ion is solvated with water molecules. The photo-reduction proceeds through the sequence of "Ligand Metal Charge Transfer (LMCT)" (chemical reactions (4)–(6)). Therefore, the photo-Fenton process can start with either the ferrous or ferric ion.

$$Fe^{2+} + H_2O_2 \rightarrow Fe^{3+} + HO^- + HO\bullet \quad (1)$$

$$Fe^{2+} + H_2O_2 \rightarrow Fe^{2+} + HO\bullet + H^+ \quad (2)$$

$$Fe^{3+} + HO\bullet + h\nu \rightarrow Fe^{2+} + HO\bullet + H^+ \quad (3)$$

$$Fe(III) - L + h\nu \rightarrow Fe(III) - L^* \quad (4)$$

$$Fe(III) - L^* \leftrightarrow Fe(II) - L' \quad (5)$$

$$Fe(II) - L' \leftrightarrow Fe(II) + L' \quad (6)$$

The objective of this study is to check the effectiveness of the photo-Fenton process, under heterogeneous and homogeneous conditions, in degrading dyes in textile wastewaters. Experiments were conducted with the Orange II compound because it is a very common textile dye; it is not biodegradable, it is included among the azo-dye groups, and it is easy to follow its primary and total degradation through spectrophotometric and COT measurements, respectively. Orange II is a very common product nowadays in the study of how to degrade it and under which conditions, so to know with a real cost-effective catalytic degradation (heterogeneous (iron fixed in perfluorinated membranes of Nafion®117) and homogeneous (dissolved iron ions) which are the best operating conditions is the aim of this study.

2. Material and Methods

2.1. Reagents

Orange II sodium salt (≥98.0%) of the acid 4-(2-hidroxy-1-naphtalene)azobenzenesulfonic (Scharlau AN0027, Scharlab, Barcelona, Spain) is an acid and monosulfated dye of the monoazo type. It has a high solubility in water due to the SO_3 group [18] and its color is due mainly to the azo group (-N=N-) [19,20].

Extrapure $FeCl_3 \cdot 6H_2O$ (Scharlau, Cod. HI0336, Barcelona, Spain) was used as source of iron ions. Hydrogen peroxide 33% w/v (Panreac, Cod. 131077. 1214, Barcelona, Spain). Other reagents were: extrapure sodium hydroxide (Scharlau, Cod. SO0420, Barcelona, Spain), sulfuric acid 95–97% (Scharlau, Cod. AC2067, Barcelona, Spain) and Milli-Q water. All the reagents were used without further purification.

Under heterogeneous conditions, two ionic exchange perfluorinated membranes of Nafion®117 (thickness 0.007 in., Sigma-Aldrich 274674, Madrid, Spain; L × An = 8 in. × 10 in.)

were used in order to fix iron (III) ions inside the photo-reactor. These membranes contain hydrophilic sulfonated groups which are immobilized in the perfluorinated structure.

The procedure used in the fixation of the iron (III) ions to the perfluorinated membranes was the following:

1. The membranes were immersed in 1 M HCl solution at 50 °C with light agitation for 30 min, and then washed with ultrapure water.
2. The membranes were then immersed in 0.3 $FeCl_3 \cdot 6H_2O$ solution during 30 min, and subsequently washed with ultrapure water. In this step, the acid hydrogen of the OH group was substituted by the iron (III) ion.
3. Finally, the membranes were introduced into a 1 M NaOH solution during 30 min to convert the iron (III) ions exchanged in their hydrated form and to ensure the same initial conditions at the beginning of each experiment. They were washed and stored with ultrapure water.
4. At the end of each experiment, the membranes were washed with ultrapure water and number 3 was repeated to regenerate the hydrated iron (III) ions.

2.2. Analytical Techniques

Spectrophotometric measurements were carried out to monitor the decoloration of the Orange II molecule, indicative of primary degradation or % decolorization, using a Jenway 6405 UV/Visible spectrophotometer, at a wavelength of 484 nm. This wavelength was chosen by other authors as the initial rate (v) of Orange II oxidation can be determined from the linear plot of absorbance versus time, using an average molar extinction coefficient of 1.8×10^4 M^{-1} cm^{-1} (484 nm) [21,22]. The TOC (total organic carbon) measurements were carried out to monitor the Orange II mineralization, indicative of the total degradation, using a Shimadzu 5050A. TOC Analyzer, Scharlab, Bacelona, Spain.

The evolution of hydrogen peroxide during the experiments was measured semi-quantitatively by means of the Merkoquant test which detects peroxides at concentrations between 1 and 100 mg/L of H_2O_2 and between 100 and 1.000 mg/L of H_2O_2 (Merck Sigma-Aldrich, 110081 and 110337, Madrid, Spain). The test is a valid colorimetric method within a pH range between 2 and 7, and responds to organic and inorganic compounds with peroxide or hydroperoxide groups.

2.3. Photo-Reactor

The photo-reactor has tubular shape and consists of a glass cylinder with entry and exit points (Figure 1). It also possesses the illumination source in its longitudinal axis. Two lamps were used: Philips TL-D 36W/18 Blue SLV centered at 440 nm, and Philips TL-D 36W/08 SLV centered at 366 nm (Philips, Madrid, Spain). The conduits between the different parts of the system were of PTFE.

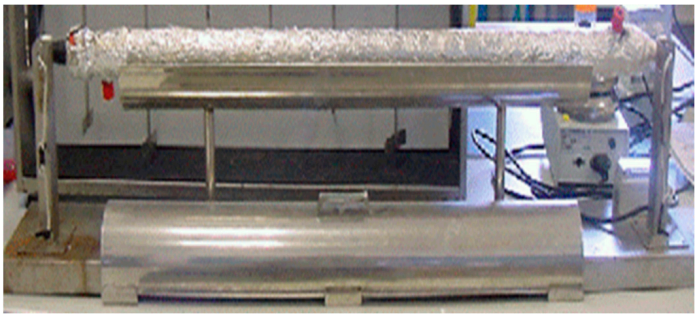

Figure 1. Schema of the photo-reactor.

The photo-reactor was operated in batch mode. Under heterogeneous conditions, the membranes with the fixed ferric ions were introduced inside the glass cylinder of the photo-reactor and adhered to the interior surface. Subsequently, the system was filled with the Orange II solution adjusted to pH 2.8 by means of H_2SO_4 (c) and NaOH 1 M. Finally,

the hydrogen peroxide was added. When the illumination source was switched on, the experiment began. The mixing flask was sealed with a reflux coolant to avoid loss by evaporation. Under homogeneous conditions, the Orange II solution with the ferric ions, adjusted to pH 2.8, and the hydrogen peroxide was prepared first. Then, this solution was introduced in the photo-reactor and again the study began when the illumination source was activated. A series of preliminary experiments were carried out to test the best pH for the study. A statistical study was then carried out to find out which parameters and the number of experiments that should be carried out to be representative.

3. Results and Discussion

3.1. Heterogeneous Catalysis

Two different experiments were carried out: one adding hydrogen peroxide continuously during the process, and the other adding it initially at the beginning of the process.

3.1.1. Continuous Addition of Hydrogen Peroxide

The hydrogen peroxide was continuously added to the reactor or mixing flask and always kept in excess. The addition was carried out slowly, in contrast with the initial input of hydrogen peroxide, in order to avoid, as far as possible, the deactivation of the hydroxyl radicals (chemical reactions (7) and (8)) by reaction with the excess of hydrogen peroxide without reacting with the iron ions or when the initiation stage has started, this could hinder the propagation stage due to deactivation among the hydroxyl radical themselves [23–25].

$$HO\bullet + HO\bullet \rightarrow H_2O_2 \quad (7)$$

$$H_2O_2 + HO\bullet \rightarrow H_2O + HO_2\bullet \quad (8)$$

Additionally, other authors suggest that an excess of hydrogen peroxide can accelerate its decomposition according to the chemical reaction (9) [26,27].

$$2H_2O_2 \rightarrow 2H_2O + O_2 \quad (9)$$

The experimental conditions at the beginning of the study were: an Orange II concentration of 0.25 mM; recirculation flow of 300 mL/min; and flow of the added hydrogen peroxide of 300 µL/min.

Wavelength (λ) of the Illumination Source

In Figure 2, the effect of the wavelength of the illumination source in primary degradation of a 0.25 mM Orange II solution can be observed. The lamps used in these tests were Philips TLD 36W718 Blue at 440 nm and TLD 36W/08 Blacklight Blue at 366 nm (Philips, Madrid, Spain). A control rehearsal in darkness (Fenton process) was also carried out.

It can be observed that the rate and percentage of degradation depend on the wavelength of the illumination source, with the best result obtained using the lamp centered at 366 nm, followed by the lamp centered at 440 nm, and the darkness control experiment (99.8, 76 and 11% after 1440 min, for 366 nm, 440 nm and darkness, respectively). At 440 nm, and consequently in darkness, the complexes of ferric ion absorb less radiation than at 366 nm, the wavelength where the photolysis of these complexes is favored, thus causing the photo-reduction of the ferric to ferrous ion. Further, an additional input of hydroxyl radicals takes place in the photo-reduction process if the ferric ion is solvated with water molecules (chemical reaction (3)) [28,29].

The influence of the intensity of the illumination source was not studied since it was found in similar studies that the degradation of Orange II solutions did not depend on the intensity of the illumination source [30]. Therefore, the wavelength of 366 nm was selected and will be used in the following assays as the most appropriate illumination source from among those studied.

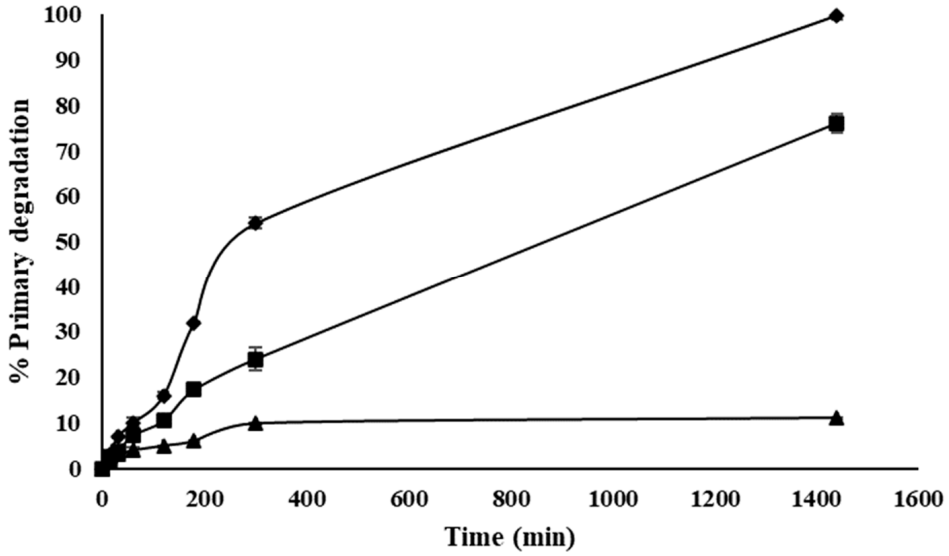

Figure 2. Percentage of primary degradation vs. time using different illumination sources: (♦) 366 nm and (■) 440 nm and (▲) darkness.

Recirculation Flow Rate

The degradation curves are obtained for the three recirculation flow rates assayed (450, 300 and 150 mL/min). It was observed that a flow rate of 450 mL/min provides the best results although after 1440 min (24 h) of reaction, similar percentages are reached with each of the three flow rates. In view of the results obtained, and from the point of view of cost, it can be concluded that the most appropriate recirculation flow rate is 300 mL/min.

Hydrogen Peroxide Flow Rate

To carry out the following study, three rates were assayed for the flow rate of hydrogen peroxide to the mixing flask: 500, 300 and 100 μL/min.

It can be observed that the degradation rate is lower for a rate of 100 μL/min of H_2O_2 than for the other two flow rates assayed and the degradation percentage after 1440 min is the lowest (92%). However, for the other two rates (300 and 500 μL/min), after 1440 min, the degradation process has been practically completed due to more hydroxyl radicals being generated by the larger inputs of hydrogen peroxide.

An input of 300 μL/min provides better results than 500 μL/min due to there being less deactivation of hydroxyl radicals with the excess of the hydrogen peroxide or among themselves (chemical reactions (7) and (8)). According to these results, the hydrogen peroxide flow rate of 300 μL/min. is considered to be best.

3.1.2. Initial Addition of Hydrogen Peroxide

These assays were carried out with the previously established values: λ = 366 nm, V_T = 1470 mL and recirculation flow rate of 300 mL/min. The dose of hydrogen peroxide was studied by varying the H_2O_2/Orange II molar relationship in accordance with the following values (R): 10, 20, 40 and 60.

In Figure 3, it can be observed that primary degradation is practically complete for all the molar relationships assayed, although it is lower for R10 (85.5 and 97.8% after 150 and 1440 min). However, the rate is higher for R40, R60 and R20 (98.9, 98.4 and 95.7% after 150 min, respectively). This result is due to the excess of hydrogen peroxide for R60, which increases the possibilities of deactivation among hydroxyl radicals or to hydrogen peroxide failing to react. In the first minutes, for R40 the degradation rate is higher than the other molar relationships although the degradation percentages rapidly increase to equal levels. Therefore, from the point of view of the consumption and hence cost of hydrogen peroxide, the best molar relationship is R20.

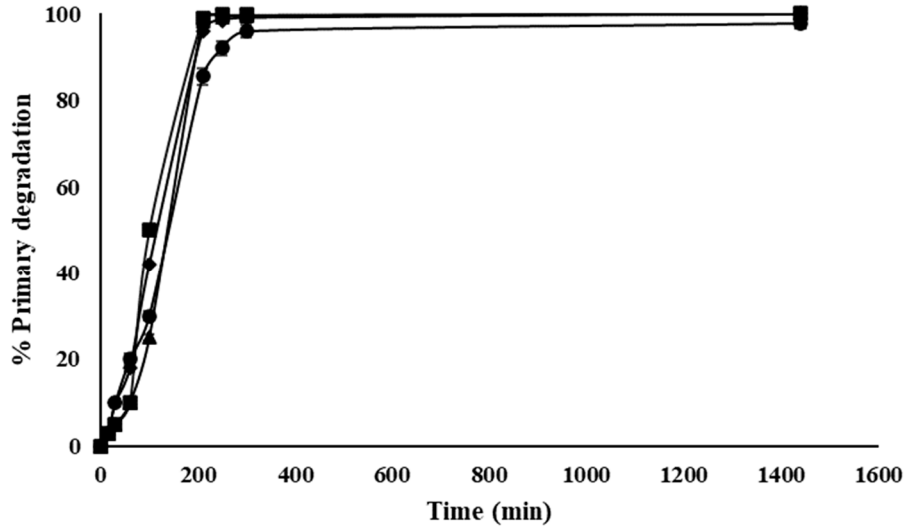

Figure 3. Percentage of primary degradation vs. time using different initial inputs of hydrogen peroxide: (♦) R60, (■) R40, (▲) R20 and (●) R10.

3.1.3. Comparison between Continuous and Initial Input of Hydrogen Peroxide

The next step is to compare the results obtained in the previous assays and to select which is the most appropriate way to add the hydrogen peroxide to the reaction [31]. The degradation percentage increases more rapidly for an initial input of hydrogen peroxide at the beginning of the process than continuous input, due to the generation of more hydroxyl radicals and in spite of the hydroxyl radical deactivation being greater with this initial method of input.

Further, the consumption of hydrogen peroxide at the end of the process is much lower where there is an input at the beginning of the process (0.2232 (0.6760) mL) than with a continuous input continuing until the end of the process (142.56 (432) mL after 1440 min). Therefore, the initial contribution was selected as the better way to add hydrogen peroxide to the reaction.

3.2. Homogeneous Catalysis

This study was carried out using a 0.25 mM Orange II solution and an R20 molar relationship added at the beginning of the assay. These experimental conditions were taken from the previous studies of photo-Fenton oxidation with the immobilized ferric ions. Thus, the variable to be optimized was the concentration of iron (III) ions in solution in the form of $FeCl_3 \cdot 6H_2O$. Four values were tested: 0, 0.5, 2 and 10 ppm. The results obtained are presented in Figure 4.

It is observed that primary degradation of the Orange II (measured by spectrophotometry at 484 nm) is practically completed in 60 min for iron concentrations of 10 and 2 ppm, 99.9% and 98.7%, respectively, although a near maximum of 97.2% was reached with 10 iron ppm after only 15 min, for 0.5 ppm, and only 90% was reached at the end of the experiment, after 100 min.

Without ferric ions, only a small degradation percentage was observed. This is due to the decomposition of the hydrogen peroxide, in absence of an iron source, being favored by the action of the illumination source and generating only a small quantity of hydroxyl radicals. This explanation is supported by the results obtained in the control experiments where Orange II resists the illumination source and does not degrade by direct action of the radiation. This result is also in agreement with the experiments carried out with textile wastewaters by Balanosky et al. [30], where a TOC decrease was observed in absence of iron (III) ions.

$$H_2O_2 \rightarrow 2HO\bullet \quad (10)$$

It can be concluded that using 2 ppm of iron (III) in solution, for approximately 60 min, it is possible to degrade almost 100% of Orange II and as well as obtaining a cost saving in comparison with 10 ppm of iron. This concentration was therefore selected as optimal.

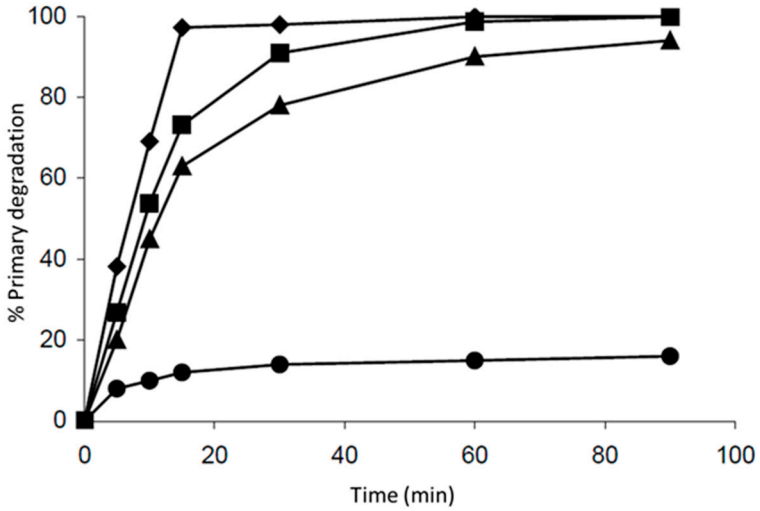

Figure 4. Percentage of primary degradation vs. time using different iron concentrations: (♦) 10 ppm, (■) 2 ppm, (▲) 0.5 ppm and (●) 0 ppm.

3.3. Mineralization, Kinetic Study and Comparison between the Two Types of Catalysis

This last part of the study has been carried out using the experimental conditions found to be most appropriate for each type of catalysis in the preceding assays. After completing the mineralization study, several different kinetic models are tested, and the two types of catalysis are compared.

3.3.1. Mineralization

Figure 5 shows the percentage of mineralization taking place under the selected conditions with each type of catalysis.

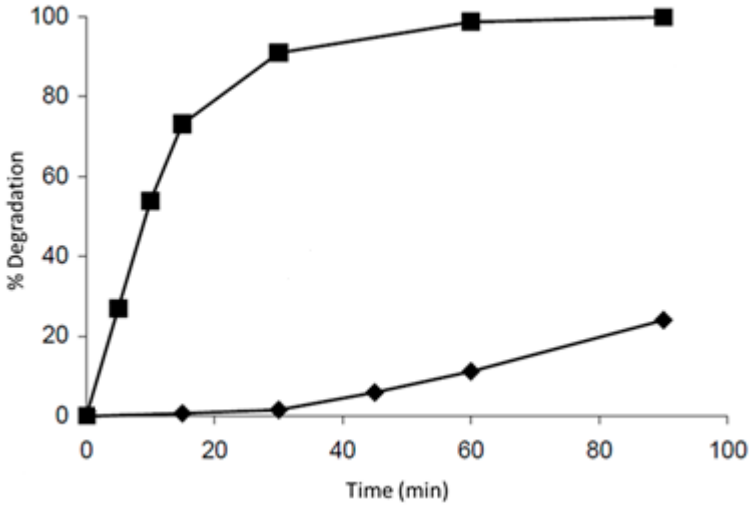

Figure 5. Evolution of the percentage degradation of Orange II by different oxidation processes: (♦) heterogeneous photo-Fenton and (■) homogeneous photo-Fenton.

Figure 5 shows the evolution of the percentage of degradation by the photo-Fenton process for both types of catalysis under equal conditions. It can be seen that under homogeneous catalysis conditions the process is much faster than under heterogeneous

catalysis—99.9 and 24% after 90 min, respectively—so it could be concluded that it is better to opt for homogeneous catalysis, especially when only 2 ppm of iron in solution is required. This is because iron is more available in the reaction medium under homogeneous catalysis conditions. The test was prolonged for the heterogeneous photo-Fenton up to 300 min, reaching 40% degradation. The results shown are largely in line with those presented by other authors showing degradations between 57% and 94% (degradation of dye under optimized conditions using heterogeneous photo-Fenton catalysts: $ZnFe_2O_4$ and GO-$ZnFe_2O_4$ composite) [32].

A novel study on the treatment of textile wastewater containing acid dye using new polymeric graphene oxide nanocomposites (GO/PAN, GO/PPy, GO/PSty) shows that after 60 min, no change in the adsorption value for the dye AO-RL was observed [33]. Considering that these processes continue to degrade, they are still more efficient.

3.3.2. Kinetic Study

To carry out the kinetic study of the mineralization results, the following kinetic models were applied: 1st order, 2nd order, and the model developed by Chan and Chu [34]. The regression coefficients obtained can be observed in Table 1. The model of Chan and Chu is selected for both types of catalysis due to the theoretical results obtained and the physical meaning of its parameters.

Table 1. Kinetic results for the different applied kinetic models.

Catalysis	1st Order	2nd Order	Chan and Chu [34]
Heterogeneus	0.8237	0.9116	0.9962
Homogeneus	0.9933	0.9631	0.9921

The equations of the model are shown below and the graphical representation is presented in Figure 6.

$$\frac{C}{C_O} = 1 - \frac{t}{\rho + \sigma t} \qquad \frac{t}{1 - C/C_O} = \rho + \sigma t$$

(**a**) (**b**)

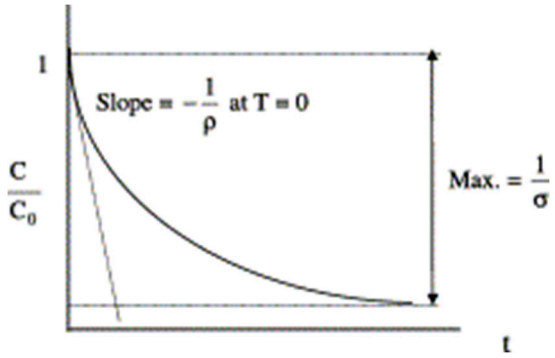

(**c**)

Figure 6. Kinetic model developed by Chan and Chu: (**a**) velocity law, (**b**) linearized velocity law and (**c**) graphical representation of the kinetic model [34].

Originally, this model was applied to the homogeneous degradation of atrazine using Fenton reagent. It describes the two stages of the reaction satisfactorily through two critical parameters: the initial slope or initial rate of the oxidation process ($-1/\rho$) and the final oxidation capacity of the oxidation process ($1/\sigma$). These parameters are sensitive to the concentration of hydrogen peroxide and iron. In order to quantitatively establish which has a higher oxidation rate and degree of mineralization, the data are presented in Table 2.

Table 2. Values obtained after fitting the experimental data with the Chan–Chu kinetic model.

	Chan and Chu [34]	
Parameters	**Heterogeneus**	**Homogeneus**
ρ (min)	266.61	60.217
$-1/\rho$ (min^{-1})	-3.75×10^{-3}	−0.0166
σ	1.5721	0.7882
$1/\sigma$	0.63	1.2687

Figure 7 shows the graphical representation obtained by applying the selected model to the experimental data. A high degree of agreement can be observed between the model and experimental data for both types of catalysis. The slopes are indicative of the higher rate and extent of mineralization under homogeneous conditions. This argument is presented in a numerical way in Table 1 where the initial capacity of oxidation, in absolute value, is higher for homogeneous catalysis.

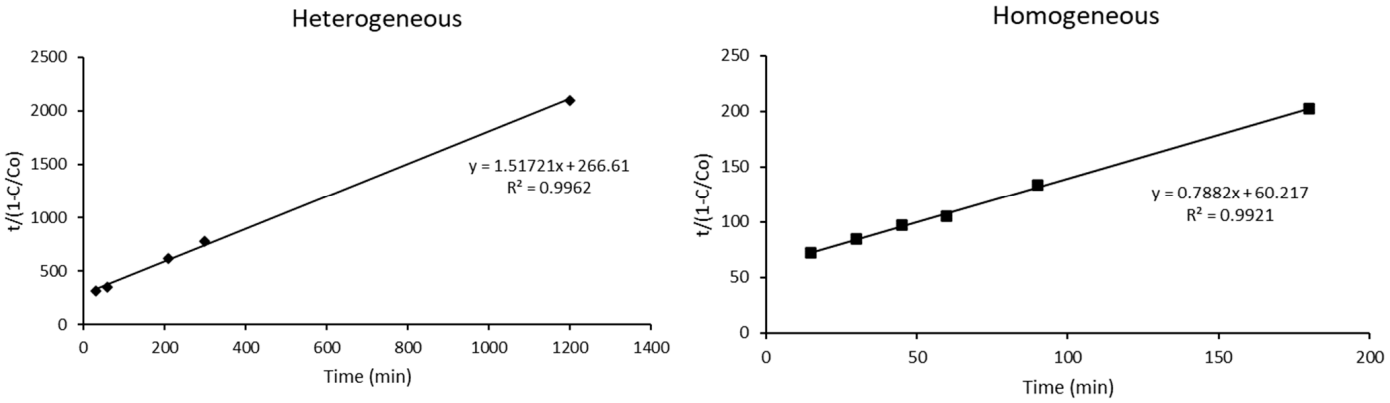

Figure 7. Linear adjustment by means of the kinetic model of Chan–Chu for (♦) heterogeneous and (■) homogeneous catalysis.

Mineralization was observed through total organic carbon, through the variable C/Co as a function of time during photo-Fenton and Orange II degradation, and the data obtained for the final oxidation capacity are in agreement with the experimental percentages of mineralization. For heterogeneous catalysis, 56% mineralization was reached whereas the model predicts 63%. This variation is logical since in the tests the iron is fixed in perfluorinated Nafion membranes and is not equally available in the reaction medium and in the solution. Here, the secondary reactions described in the section on the Chan–Chu kinetic model become important. Nevertheless, the correlation between the experimental and model-predicted oxidation capacities is acceptable.

Regarding homogeneous catalysis, according to the model, 100% mineralization is reached because $(1/\sigma)$ takes a value greater than 1 since the model calculates it on infinite time. This result is in agreement with the experimental data after 300 min where the percentage of mineralization reached was close to 100%. A total of 100% should have been mineralized, which does not occur because there are secondary reactions already mentioned that become important at low concentrations as is the case of perfluorinated membranes.

3.3.3. Comparison between the Two Types of Catalysis

The photo-Fenton process is more effective under homogeneous than heterogeneous catalysis conditions in primary degradation and mineralization, due to the greater availability of the iron in homogeneous catalysis for reacting with the hydrogen peroxide. This was demonstrated in the preceding assays.

4. Conclusions

The photo-Fenton process is more effective with an initial input of hydrogen peroxide than with a continuous input until the end of the process. Nevertheless, the photo-Fenton process takes place effectively under heterogeneous and homogeneous catalysis conditions. The process is much faster under homogeneous conditions than under heterogeneous conditions, in primary degradation (decolorization) and in mineralization (CO_2 and H_2O), due to the greater availability of iron in the reaction. The main difference between the two types of catalysis is the status of the iron: fixed in heterogeneous and in solution in homogeneous catalysis. Except for this difference, the experimental conditions identified as most appropriate are common for both processes. Under homogeneous catalysis conditions, the process is much faster than under heterogeneous catalysis—99.9 and 24% after 90 min, respectively—so it could be concluded that it is better to opt for homogeneous catalysis, especially when only 2 ppm of iron in solution is required.

The kinetic model that best describes both types of catalysis is the model developed by Chan and Chu in 2003. It is also considered that the physical parameters described in this model contribute to a better understanding and explanation of the different stages of the process. Conditional upon extrapolation to the pilot scale, it can be concluded that the photo-Fenton process is capable of effectively eliminating dyes from textile industry wastewaters.

Author Contributions: Conceptualization, A.R.-F., M.A.M. and J.M.Q.; methodology, A.R.-F.; investigation, A.R.-F., M.A.M. and J.M.Q.; resources, M.A.M. and J.M.Q.; data curation, A.E.-C. and J.M.Q.; writing—original draft preparation, A.R.-F., A.E.-C., M.A.M. and J.M.Q.; writing—review and editing, A.E.-C. and J.M.Q. All authors have read and agreed to the published version of the manuscript.

Funding: This research received no external funding.

Data Availability Statement: The authors confirm that the data supporting the findings of this study are available within the article.

Conflicts of Interest: The authors declare no conflict of interest.

References

1. Benkhaya, S.; M'rabet, A.; El Harfi, A. A review on classifications, recent synthesis and applications of textile dyes. *Inorg. Chem. Commun.* **2020**, *115*, 107891. [CrossRef]
2. Vandevivere, P.C.; Bianchi, R.; Verstraete, W. Treatment and reuse of wastewater from the textile wet-processing industry: Review of emerging technologies. *J. Chem. Technol. Biotechnol.* **1998**, *72*, 289–302. [CrossRef]
3. Gadekar, M.R.; Ahammed, M.M. Use of water treatment residuals for colour removal from real textile dye wastewater. *Appl. Water Sci.* **2020**, *10*, 160. [CrossRef]
4. Kuo, W.G. Decolorizing dye wastewater with Fenton's reagent. *Water Res.* **1992**, *26*, 881–886. [CrossRef]
5. Mohamed, R.M.S.R.; Nanyan, N.M.; Rahman, N.A.; Kutty, N.M.A.I.; Kassim, A.H.M. Colour removal of reactive dye from textile industrial wastewater using different types of coagulants. *Asian J. Appl. Sci.* **2014**, *2*, 650–657.
6. Hoffmann, M.; Martin, S.; Choi, W.; Bahnemann, D. Environmental applications of semiconductor photocatalysis. *Chem. Rev.* **1995**, *95*, 69. [CrossRef]
7. Pitter, P.; Chudoba, J. *Biodegradability of Organic Substances in the Aquatic Environment*; CRC Press: Boca Raton, FL, USA, 1990.
8. Little, L.W.; Lamb, J.C.; Chillingworth, M.A.; Durkin, W.B. Acute toxicity of selected commercial dyes to the fathead minnow and evaluation of biological treatment for reduction of toxicity. In Proceedings of the 29th Industrial Waste Conference, West Lafayette, IN, USA, 7–9 May 1977.
9. Howard, P.H. *Handbook of Environmental Degradation Rates, Lewis*; CRC Press: Washington, DC, USA, 1989.
10. Kusic, H.; Juretic, D.; Koprivanac, N.; Marin, V.; Božić, A. Photooxidation processes for an azo dye in aqueous media: Modeling of degradation kinetic and ecological parameters evaluation. *J. Hazard. Mater.* **2011**, *185*, 1558–1568. [CrossRef]
11. Rupert, G.; Bauer, R.; Heisler, G. The Photo-Fenton reaction—An effective photochemical wastewater treatment process. *J. Photochem. Photobiol. A Chem.* **1993**, *73*, 75–78. [CrossRef]
12. Bauer, R.; Fallmann, H. The Photo-Fenton oxidation—A cheap efficient wastewater treatment method. *Res. Chem. Intermed.* **1997**, *23*, 341–354. [CrossRef]
13. Coulibaly, G.N.; Bae, S.; Kim, J.; Assadi, A.A.; Hanna, K. Enhanced removal of antibiotics in hospital wastewater by Fe–ZnO activated persulfate oxidation. *Environ. Sci. Water Res. Technol.* **2019**, *5*, 2193–2201. [CrossRef]
14. Xiong, H.; Shi, K.; Han, J.; Cui, C.; Liu, Y.; Zhang, B. Synthesis of β-FeOOH/polyaniline heterogeneous catalyst for efficient photo-Fenton degradation of AOII dye. *Environ. Sci. Pollut. Res. Int.* **2023**, *30*, 59366–59381. [CrossRef]

15. Wang, F.; Zhang, Y.; Ming, H.; Wang, L.; Zhao, Z.; Wang, Y.; Liang, J.; Qin, J. Degradation of the ciprofloxacin antibiotic by photo-Fenton reaction using a Nafion/iron membrane: Role of hydroxyl radicals. *Environ. Chem. Lett.* **2020**, *18*, 1745–1752. [CrossRef]
16. Xu, Y.; Guo, X.; Zha, F.; Tang, X.; Tian, H. Efficient photocatalytic removal of orange II by a Mn3O4–FeS2/Fe2O3 heterogeneous catalyst. *J. Environ. Manag.* **2020**, *253*, 109695. [CrossRef]
17. Fenton, H.J.H. Oxidation of tartaric acid in presence of iron. *J. Chem. Soc.* **1894**, *65*, 899–910. [CrossRef]
18. Zhu, W.; Yang, Z.; Wang, L. Application of ferrous hydrogen peroxide for treatment of DSD-acid manufacturing process wastewater. *Water Res.* **2001**, *35*, 2087–2091. [CrossRef]
19. Zollinger, H. *Color Chemistry: Synthesis, Properties and Applications of Organic Dyes and Pigments*; VCH Publishers: New York, NY, USA, 1987.
20. Augugliaro, V.; Baiocchi, C.; Bianco-Prevot, A.; Garcia-Lopez, E.; Loddo, V.; Malato, S.; Marci, G.; Palmisano, L.; Pazzi, M.; Pramauro, E. Azo-dyes photocatalytic degradation in aqueous suspension of TiO_2 under solar irradiation. *Chemosphere* **2002**, *49*, 1223–1230. [CrossRef]
21. Pourreza, N.; Zareian, M. Determination of Orange II in food samples after cloud point extraction using mixed micelles. *J. Hazard Mater.* **2009**, *165*, 1124–1127. [CrossRef]
22. Wang, X.; Xu, B.; Liu, Z. The oxidase-like activity of hemin encapsulated by single-ring GroEL mutant and its application for colorimetric detection. *J. Mater. Sci.* **2018**, *53*, 8786–8794. [CrossRef]
23. Cuerda-Correa, E.M.; Alexandre-Franco, M.F.; Fernández-González, C. Advanced Oxidation Processes for the Removal of Antibiotics from Water. An Overview. *Water* **2020**, *12*, 102. [CrossRef]
24. Walling, C. Fenton's reagent revisited. *Acc. Chem. Res.* **1975**, *8*, 125–131. [CrossRef]
25. Sychev, A.Y.; Isak, V.G. Iron compounds and the mechanisms of the homogeneous catalysis of the activation of O_2 and H_2O_2 and the activation of organic substrates. *Russ. Chem. Rev.* **1995**, *64*, 1105–1129. [CrossRef]
26. Feuerstein, W.; Gilbert, D.; Eberle, S.H. Model experiments for the oxidation of aromatic compounds by hydrogen peroxide in waste water treatment. *Vom Wasser* **1981**, *56*, 35–54.
27. Kim, S.M.; Geissen, S.U.; Vogelpohl, A. Landfill leachate treatment by a photo assisted Fenton reaction. *Water Sci. Technol.* **1997**, *35*, 239–248. [CrossRef]
28. Walling, C.; Amranth, K. Oxidation of mandelic acid by Fenton's reagent. *J. Am. Chem. Soc.* **1982**, *104*, 1185–1189. [CrossRef]
29. Faust, B.C. A review of the photochemical redox reactions oh iron(III) species in atmospheric, oceanic and surface waters: Influence on geochemical cycles and oxidant formation. In *Aquatic and Surface Photochemistry*; Helz, G.R., Zepp, R.G., Crosby, D.G., Eds.; Lewis Publishers: Boca Ratonn, FL, USA, 1994; Chapter 1.
30. Balanosky, E.; Herera, F.; Lopez, A.; Kiwi, J. Oxidative degradation of textile waste water. Modeling reactor performance. *Water Res.* **2000**, *34*, 582–596. [CrossRef]
31. Lopez, C.; Lema, J.M.; Moreira, M.T. Oxidación del Tinte azo Orange II Mediante MnP en Reactores Enzimáticos Operados en Continuo. Ph.D. Thesis, Universidad de Santiago de Compostela, Galicia, Spain, 2005.
32. Nadeem, N.; Zahid, M.; Tabasum, A.; Mansha, A.; Jilani, A.; Bhatti, I.A.; Bhatti, H.N. Degradation of reactive dye using heterogeneous photo-Fenton catalysts: $ZnFe_2O_4$ and GO-$ZnFe_2O_4$ composite. *Mater. Res. Express* **2020**, *7*, 015519. [CrossRef]
33. Noreen, S.; Tahira, M.; Ghamkhar, M.; Hafiz, I.; Bhatti, H.N.; Nadeem, R.; Murtaza, M.A.; Yaseen, M.; Sheikh, A.A.; Naseem, Z.; et al. Treatment of textile wastewater containing acid dye using novel polymeric graphene oxide nanocomposites (GO/PAN, GO/PPy, GO/PSty). *J. Mater. Res. Technol.* **2021**, *14*, 25–35. [CrossRef]
34. Chan, K.H.; Chu, W. Modeling the reaction kinetics of Fenton's process on the removal of atrazine. *Chemosphere* **2003**, *51*, 305–311. [CrossRef]

Disclaimer/Publisher's Note: The statements, opinions and data contained in all publications are solely those of the individual author(s) and contributor(s) and not of MDPI and/or the editor(s). MDPI and/or the editor(s) disclaim responsibility for any injury to people or property resulting from any ideas, methods, instructions or products referred to in the content.